Top-down Fabricated microPlates for Prolonged, Intra-articular Matrix Metalloproteinase 13 siRNA Nanocarrier Delivery to Reduce Post-Traumatic Osteoarthritis

Authors: *Sean K Bedingfield[1†], Juan M. Colazo[1, 2, 3†], Martina Di Francesco[4†], Fang Yu[1], Danielle D. Liu[1, 2, 3], Valentina Di Francesco[4], Lauren E. Himmel[5], Mukesh K. Gupta[1], Hongsik Cho[6, 7], Karen A. Hasty[6, 7], Paolo Decuzzi[4], and Craig L. Duvall[1*]*

1. Department of Biomedical Engineering, Vanderbilt University, Nashville, TN 37232.
2. Vanderbilt University School of Medicine, Vanderbilt University, Nashville, TN 37232.
3. Medical Scientist Training Program, Vanderbilt University School of Medicine, Nashville, TN 37232.
4. Laboratory of Nanotechnology for Precision Medicine, Istituto Italiano di Tecnologia, Via Morego 30, Genoa 16163, Italy
5. Department of Pathology, Microbiology and Immunology, Vanderbilt University Medical Center, Nashville, TN 37232.
6. Department of Orthopaedic Surgery and Biomedical Engineering, University of Tennessee Health Science Center-Campbell Clinic, Memphis TN 38104.
7. Research 151, VA Medical Center, 1030 Jefferson Ave., Memphis, TN 38104.

[†]Contributed equally to this work; Co-first authors

[*] Corresponding author: Craig L. Duvall, PhD, craig.duvall@vanderbilt.edu

Craig L. Duvall, Ph.D.
Cornelius Vanderbilt Chair
Professor and Director of Undergraduate Studies, Biomedical Engineering
Professor, Ophthalmology and Visual Sciences
Vanderbilt University
email: craig.duvall@vanderbilt.edu
office phone: (615)322-3598
fax: (615)343-7919
web: https://my.vanderbilt.edu/duvall/
Follow us on Twitter: @Duvall_Lab_VU

Office: Engineering and Science Building Rm. 444

Mailing Address:
5824 Stevenson Center
Nashville, TN 37232

Cy5-DNA, MW = 14617.9 g/mole Antisense: 5'-/5Cy5/GATGACCAGTTTCTATTTCTGAC-3', MW = 7537.2 g/mole Sense: 5'-GTCAGAAATAGAAACTGGTCATC-3', MW = 7080.7 g/mole
Luciferase siRNA (siLUC), MW = 16381.1 g/mole Antisense: 5'-mG/i2FA/mC/i2FA/mU/i2FU/mU/i2FC/mG/i2FA/mA/i2FG/mU/i2FA/mU/i2FU/mC/i2FC/mG/i2FC/mG/i2FU/mA/i2FC/mG/i2FU/mG-3', MW = 8832.4 g/mole Sense: 5'- /52FC/mG/i2FU/ mA/i2FC/mG /i2FC/mG/i2FG/ mA/i2FA/mU /i2FA/mC/i2FU/ mU/i2FC/mG /i2FA/mA/i2FA/ mU/32FG/ -3', 7548.7 g/mole
Negative Control siRNA (siNEG), MW = 13661.4 g/mole Antisense: 5'-mA/i2FU/mA/i2FC/mG/i2fC/mG/i2FU/mA/i2FU/mU/i2FA/mU/i2FA/mC/i2FG/mC/i2FG/mA/i2FU/mU-3', MW = 6832.2 g/mole Sense: 5''-/52FA/mA/i2FU/ mC/i2FG/mC /i2FG/mU/i2FA/ mU/i2FA/mA /i2FU/rA/i2FC/ mG/i2FC/mG /i2FU/mA/32FU/-3', MW = 6829.2 g/mole
MMP13 siRNA (siMMP13), MW = 13615.3 g/mole Antisense: 5'-mA/i2FU/mG/i2FG/mU/i2FC/mC/i2FC/mA/i2FA/mA/i2FC/mG/i2FA/mA/i2FC/mU/i2FU/mA/i2FU/mU-3', MW = 6815.2 g/mole Sense: 5'-/52FU/mA/i2FA/ mG/i2FU/mU /i2FC/mG/i2FU/ mU/i2FG/mG /i2FG/rA/i2FC/ mC/i2FA/mU /i2FU/mU/32FU/-3', 6800.1 g/mole

Table S1. Nucleic acid sequences used with corresponding molecular weight (MW) (m = 2'-O-methylation; i2F = 5-Iodo-2'-Fluoro nucleoside; 52F = 5' initiating 2'-Fluoro; 32F = 3' terminating 2'-Fluoro).

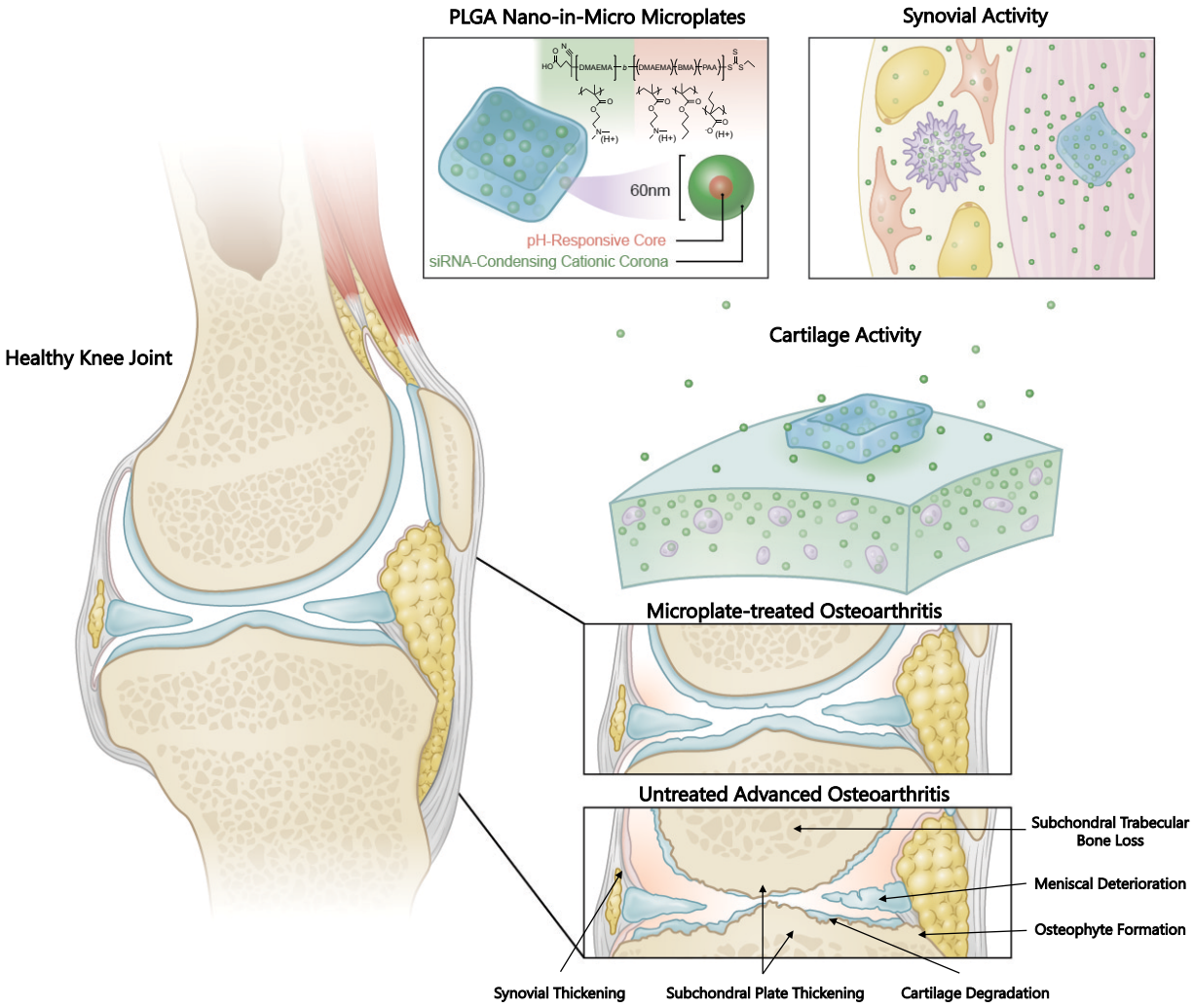

Supplemental Figure 1. Conceptual illustration of nano-in-micro approach for sustained siRNA delivery for the treatment of PTOA. (Left) Representation of a healthy knee sagittal cross-section. (Top-Center) Nano-in-micro formulation of PLGA microPlates (μPLs) containing endosomolytic siRNA nanoparticles (siNP-μPLs). (Top-Right/Center) Nanoparticle (NPs) release from the microPlates (μPLs) to achieve delivery throughout the joint. (Bottom-Right) Representation of microPlate-treated (siNP-μPLs) *versus* untreated, advanced osteoarthritis. The authors acknowledge Lauren Hugdahl for assistance with the illustration of this figure.

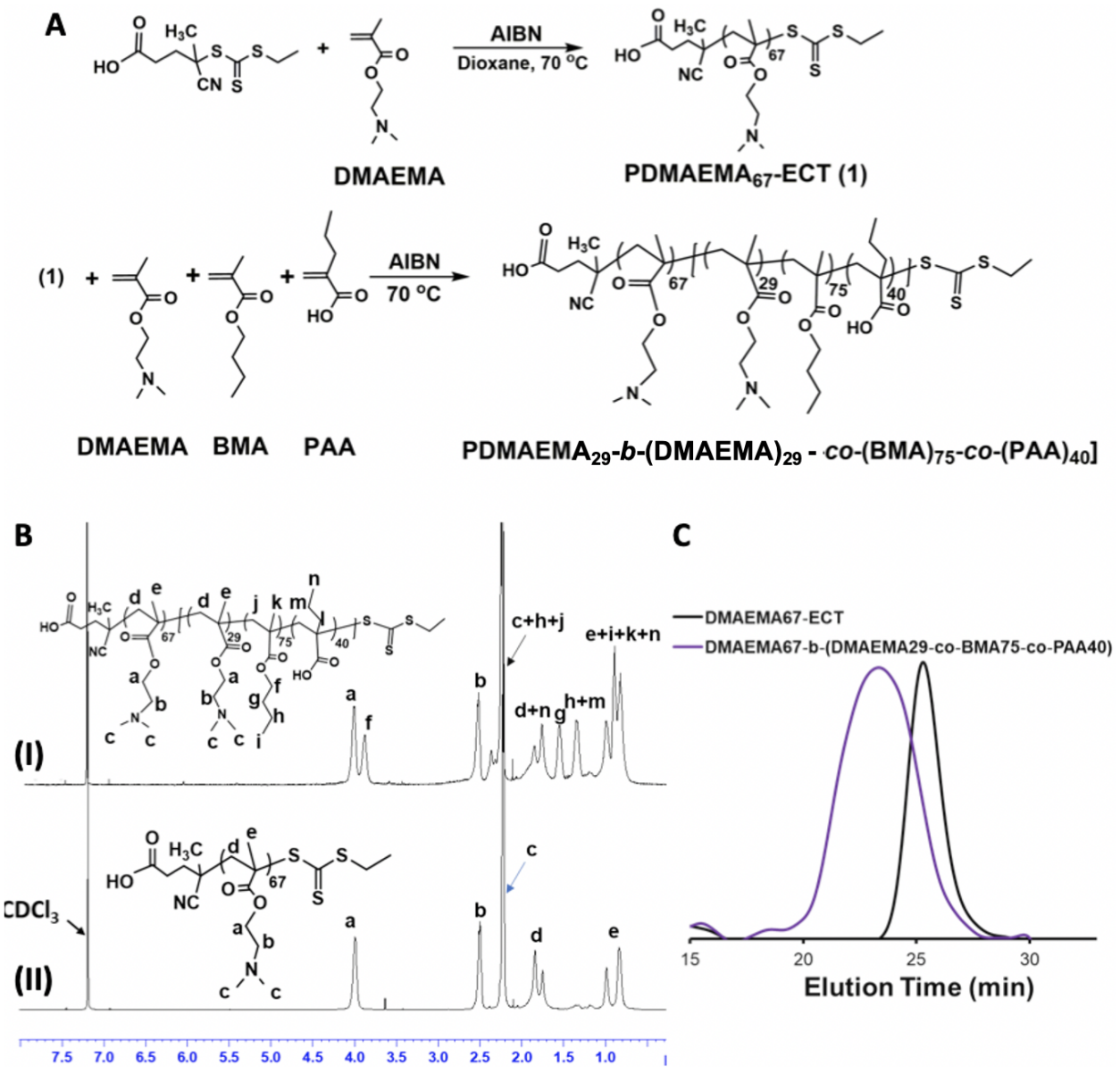

Supplemental Figure 2: Chemical synthesis and characterization of the diblock copolymer of PDMAEMA$_{67}$-b-P(DMAEMA$_{29}$-co-PAA$_{40}$-co-BMA$_{75}$) **A**. Chemical schematic for the synthesis of the diblock copolymer of poly(DMAEMA)$_{67}$-b-P(DMAEMA$_{29}$-co-BMA$_{75}$-co-PAA$_{40}$) by reversible addition fragmentation chain transfer (RAFT) polymerization. **B**. ^{1}H NMR spectra of (I) poly(DMAEMA)$_{67}$-ECT, and (II) poly(DMAEMA)$_{67}$-b-P(DMAEMA$_{29}$-co-PAA$_{40}$-co-BMA$_{75}$) in $CDCl_3$. **C**. GPC based refractive index (RI) traces of PDMAEMA$_{67}$ macro-CTA, and PDMAEMA$_{67}$-b-P(DMAEMA$_{29}$-co- PAA$_{40}$-co-BMA$_{75}$).

A

Characterization of siNPs

Sample	Size (nm)	PDI	EE% ± Std Dev
Empty-NPs	61.07 ± 0.3	0.10	----
siLuc-NPs	60.42 ± 5.6	0.15	93.8 ± 16.3
siMMP13-NPs	60.22 ± 0.4	0.05	88.0 ± 21.0

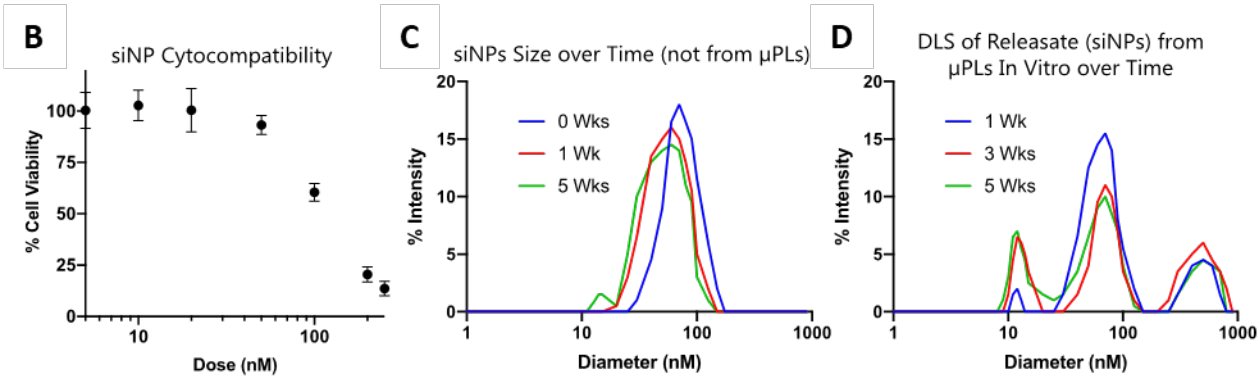

Supplemental Figure 3: Characterization of siNP cytocompatibility and stability over time in solution and in releasates from µPLs. A. Sizing by DLS and RNA encapsulation efficiency for empty, siLUC-, and siMMP13-NPs. Data are expressed as the mean (n = 3) ± SD; **B.** siNP dose-dependent toxicity study in chondrogenic ATDC5 cells; **C.** Representative DLS of siNPs left at 37ºC over time; **D.** Dynamic light scattering (DLS) on releasates from µPLs collected at 1, 3, and 5 weeks. Error bars represent standard error.

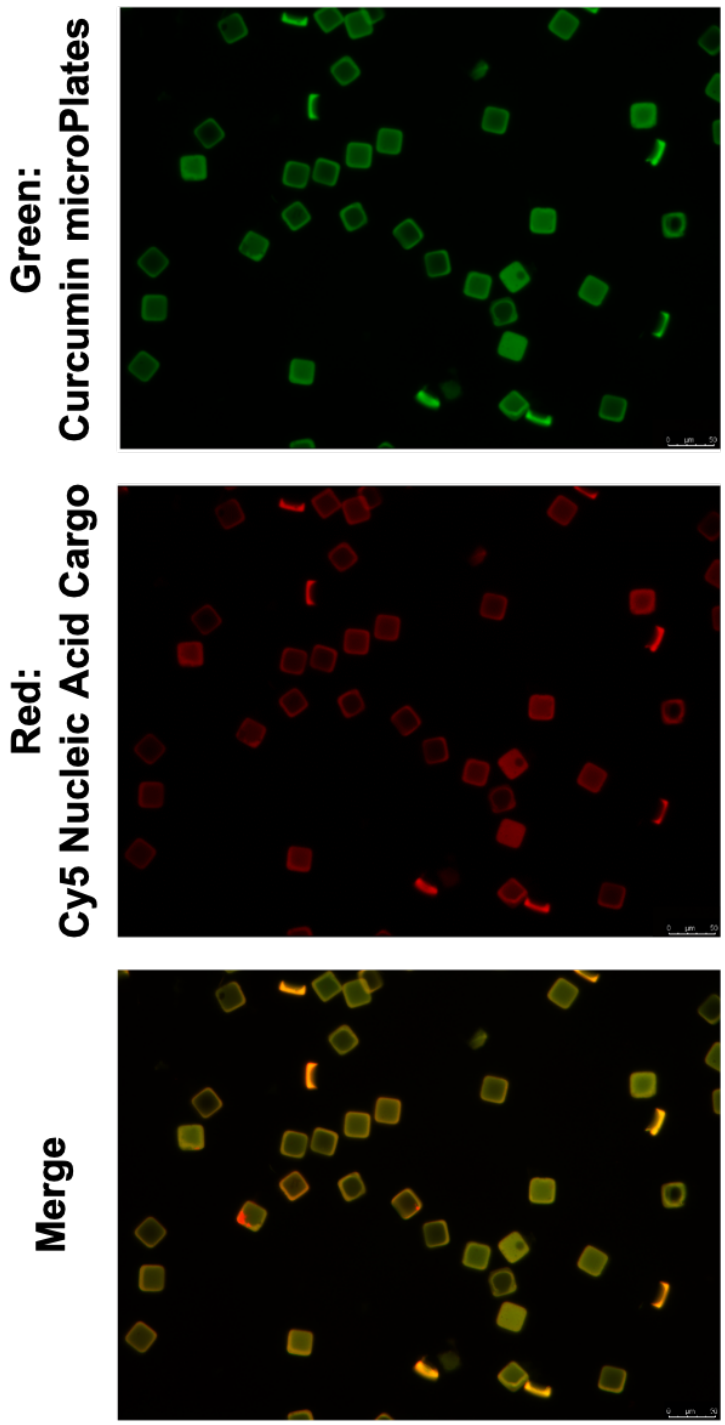

Supplemental Figure 4: Fluorescence microscopy of Cy5-siNP-µPLs separated into the green curcumin channel (PLGA microPlates), the red Cy5 channel (nucleic acid cargo), and both channels (merge) demonstrate efficient and dispersed loading of the nucleic acid cargo (red) within the PLGA microPlates (green).

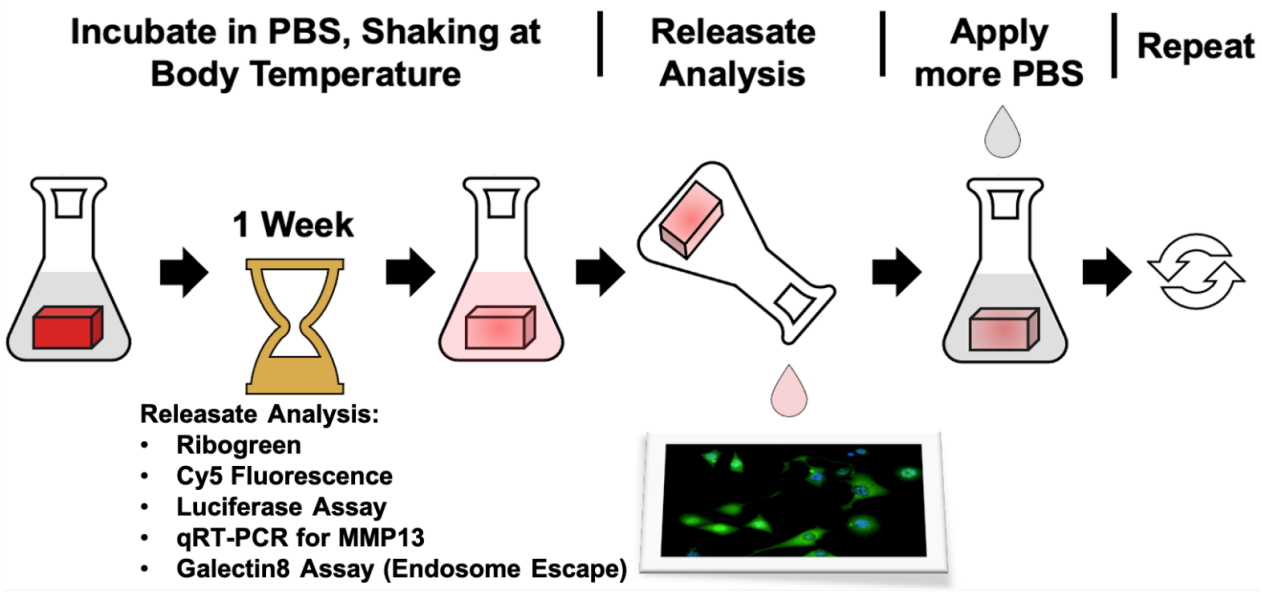

Supplemental Figure 5: Graphical representation of the *in-vitro* microplate releasate study and assays performed.

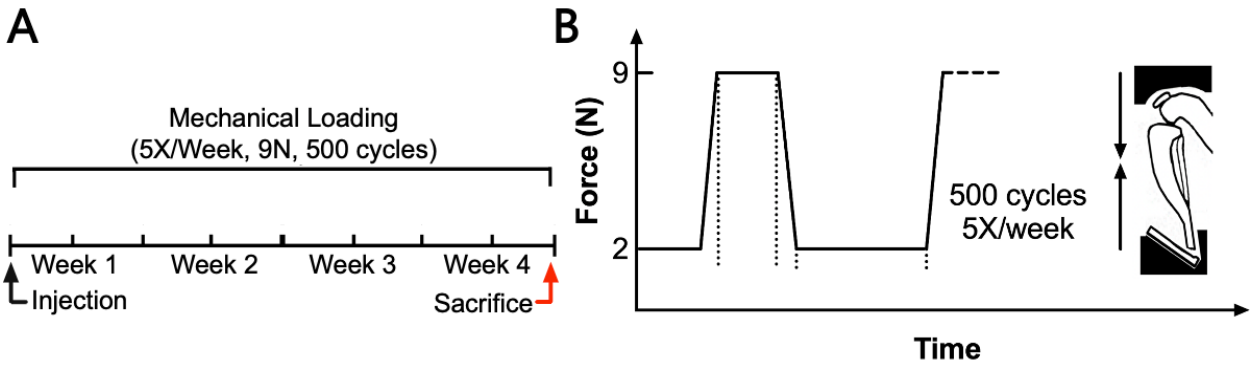

Supplemental Figure 6: A. Timeline of joint loading and treatment used in therapeutic PTOA studies; **B.** Graphical representation of the repeated mechanical load applied and compressed to the flexed mouse knee joints for induction of murine post-traumatic osteoarthritis.

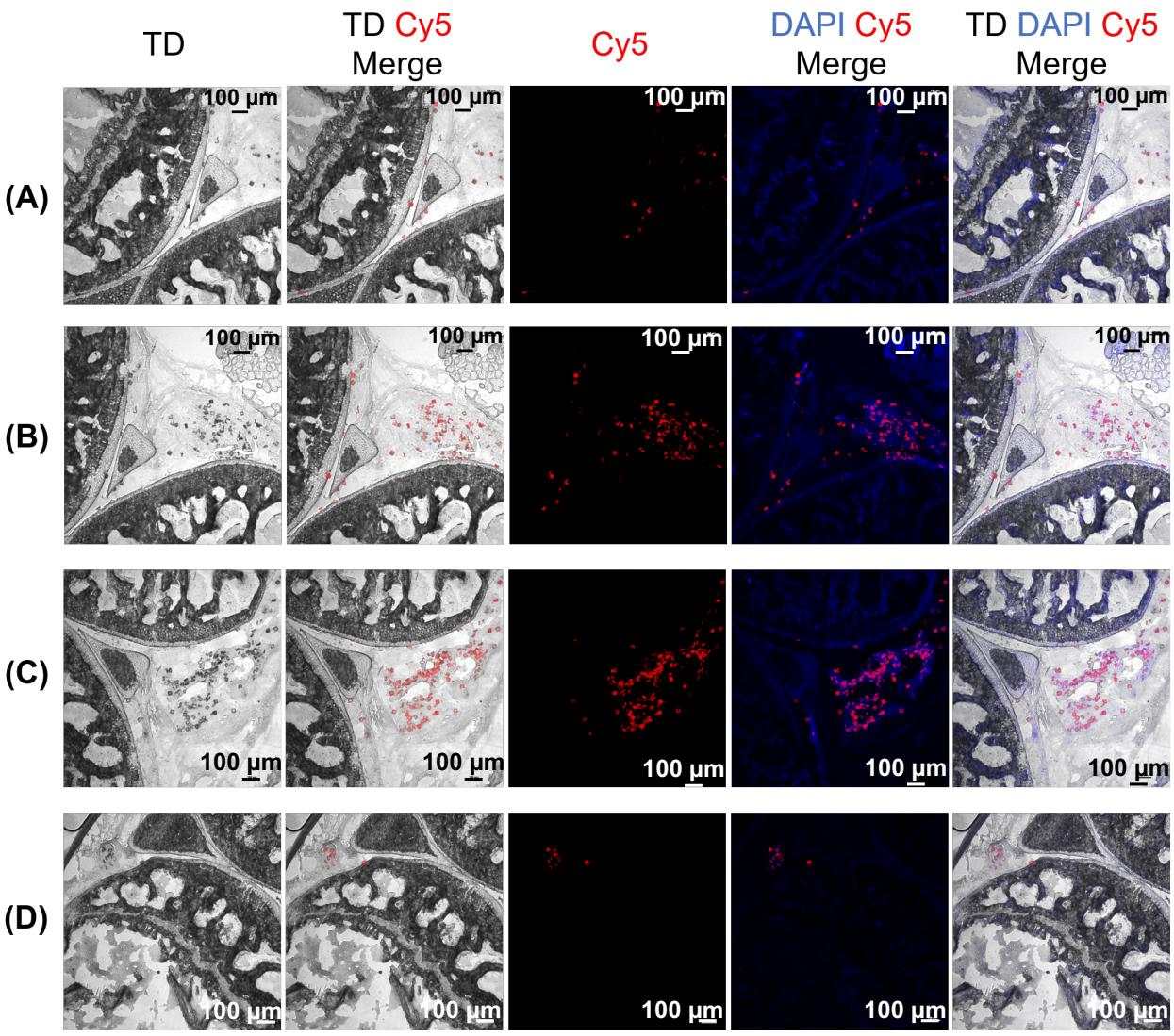

Supplemental Figure 7: Confocal microscopy (10x magnification) of the knee joint 1 day after intra-articular injection of Cy5-siNP-µPLs in a PTOA mouse model. Cy5-siNP-µPLs reach the femoral-tibial cartilage interface (**A**), the synovium/infrapatellar fat pad (**B,C**) and can be seen deposited in the posterior joint space (**D**); TD = transmitted detector.

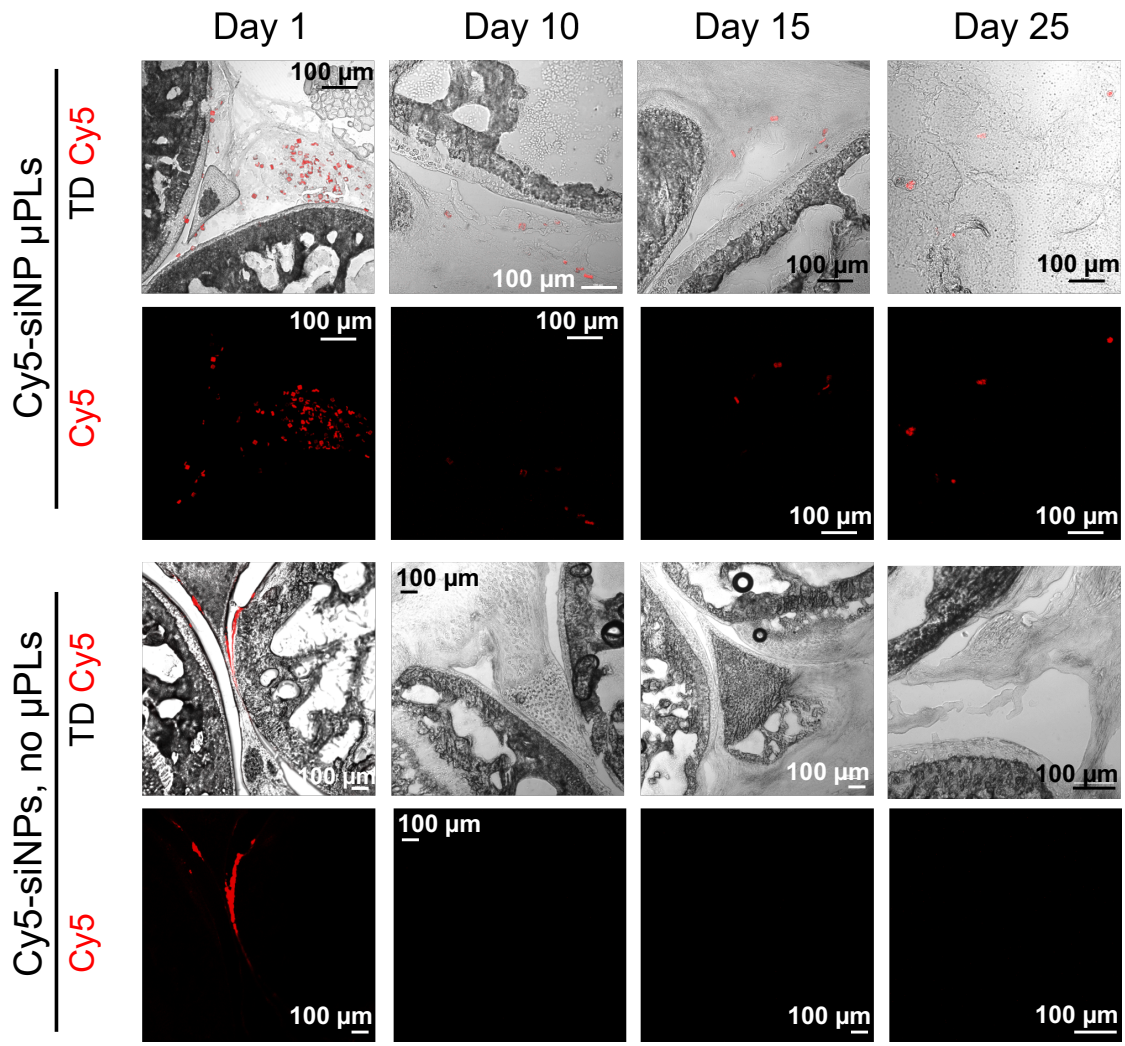

Supplemental Figure 8: Confocal microscopy imaging time course comparison of Cy5-siNP-µPLs *vs.* free Cy5-siNPs over 25 days in a PTOA mouse model. Imaging settings were controlled to be the same for all images displayed for a given timepoint but not across different timepoints in the interest of resolving the residual particles at late timepoints without causing signal saturation at early timepoints. The Cy5-siNP-µPLs were visualized across all 25 days, while free Cy5-siNPs were only detected 1 day after injection. Furthermore, free siNPs (cationic) were mostly seen on the articular cartilage surface and were not seen in other important joint tissues, most likely due to electrostatic interactions with cartilage combined with rapid lymphatic drainage of smaller NPs from the joint. TD = transmitted detector.

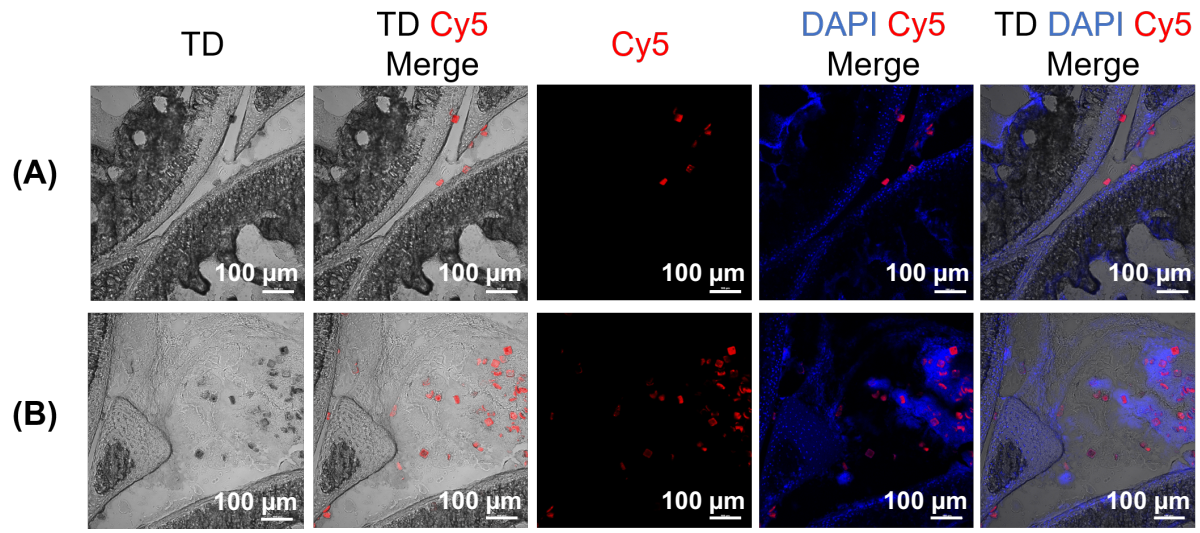

Supplemental Figure 9: Confocal microscopy (20x magnification) of the knee joint 1 day after intra-articular injection of Cy5-siNP-µPLs in a PTOA mouse model. A. Cy5-siNP-µPLs deposited at the femoral-tibial cartilage interface; **B.** Cy5-siNP-µPLs deposited near the meniscus and within the synovium / infrapatellar fat pad; TD = transmitted detector.

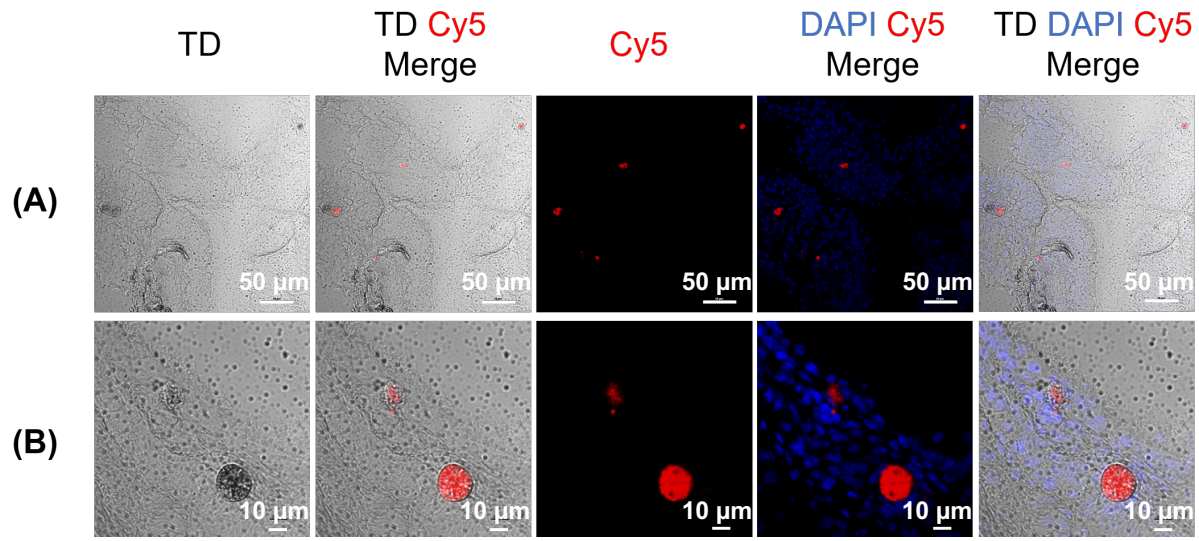

Supplemental Figure 10: Confocal microscopy (20x magnification) of the knee joint 25 days after intra-articular injection of Cy5-siNP-µPLs in a PTOA mouse model. A. Cy5-siNP-µPLs are still present in intra-articular tissues, but are losing structure, shape, and fluorescent intensity at day 25 as PLGA degrades; **B.** An instance of apparent aggregation of remnants of Cy5-siNP-µPLs was detectable at day 25. Cy5-siNP-µPLs at day 25; TD = transmitted detector.

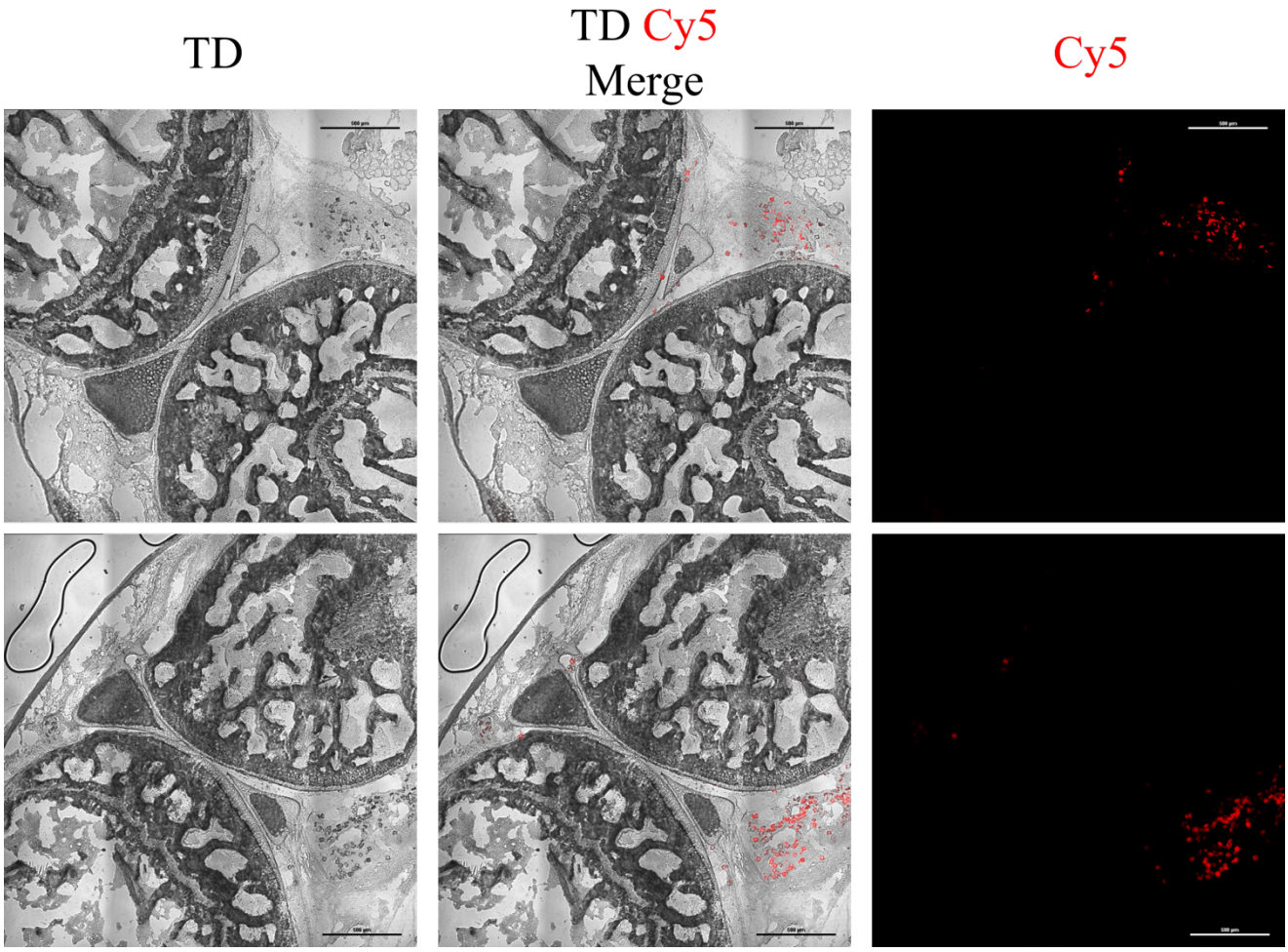

Supplemental Figure 11: Whole mouse joint images at Day 1 after Intra-articular injection demonstrating dispersion of the nano-in-micro system (Cy5-siNPs/μPLs) across the entire knee joint tissue without being found in surrounding musculature or subchondral bone regions of the tissue. TD = transmitted detector.

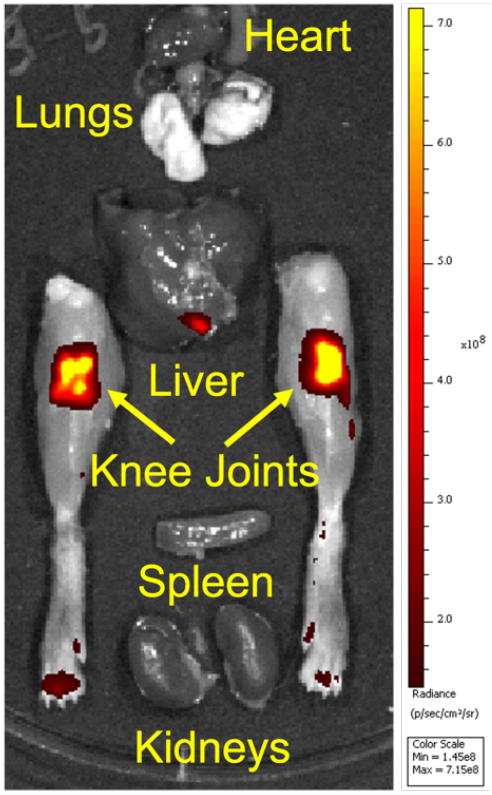

Supplemental Figure 12: Cy5 signal biodistribution at Day 1 after Intra-articular injection of the nano-in-micro system (Cy5-siNPs/µPLs) demonstrating relative localization of signal to the knee joint tissue without being found in organs such as the heart, lungs, liver, spleen, and kidneys.

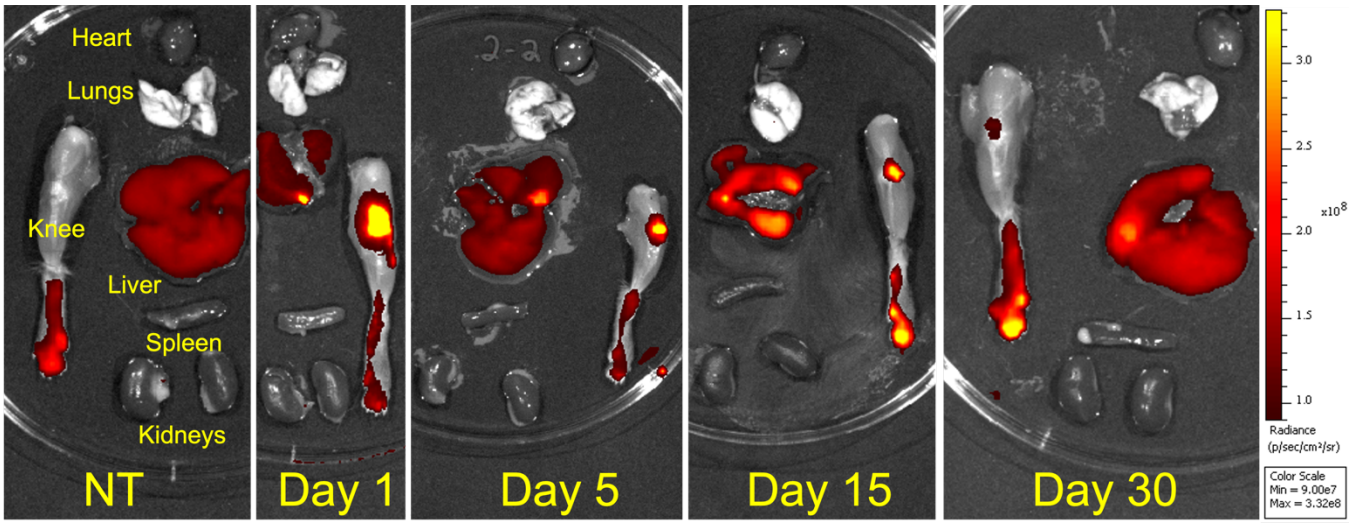

Supplemental Figure 13. Cy5 signal biodistribution over time after intra-articular injection of the nano-in-micro system (Cy5-siNPs/µPLs) demonstrating persistent localization of signal to the knee joint tissue without detectable signal in organs such as the heart, lungs, spleen, and kidneys. There is potentially minimal clearance occurring through the liver, though it is not significantly above background autofluorescence of this organ. Note that the paw and liver autofluorescence is also seen in the no treatment mice (NT) with no Cy5 signal localizing to the knee of the NT mice.

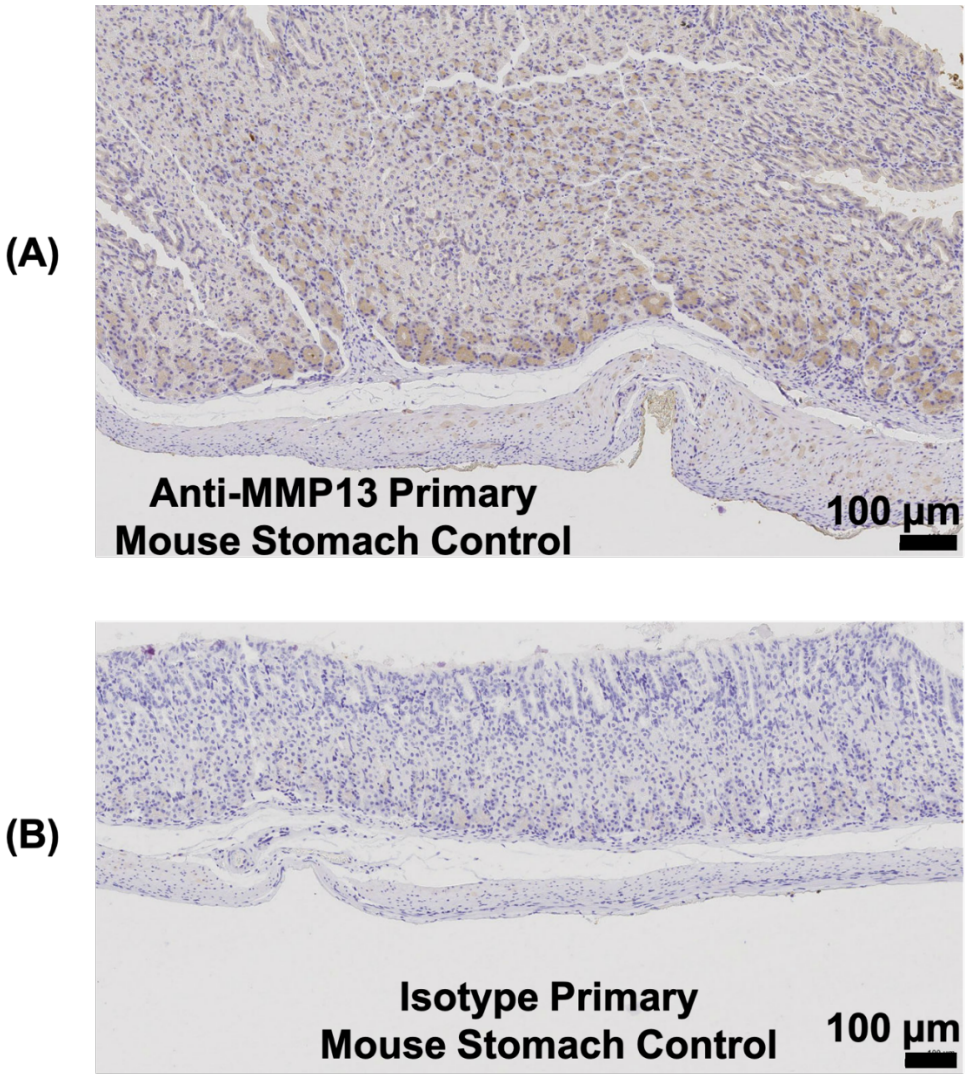

Supplemental Figure 14: (A) Positive control (anti-MMP13 primary antibody) and (B) negative control (isotype primary antibody) staining on mouse stomach tissue done to validate mouse MMP13 immunohistochemistry protocols.

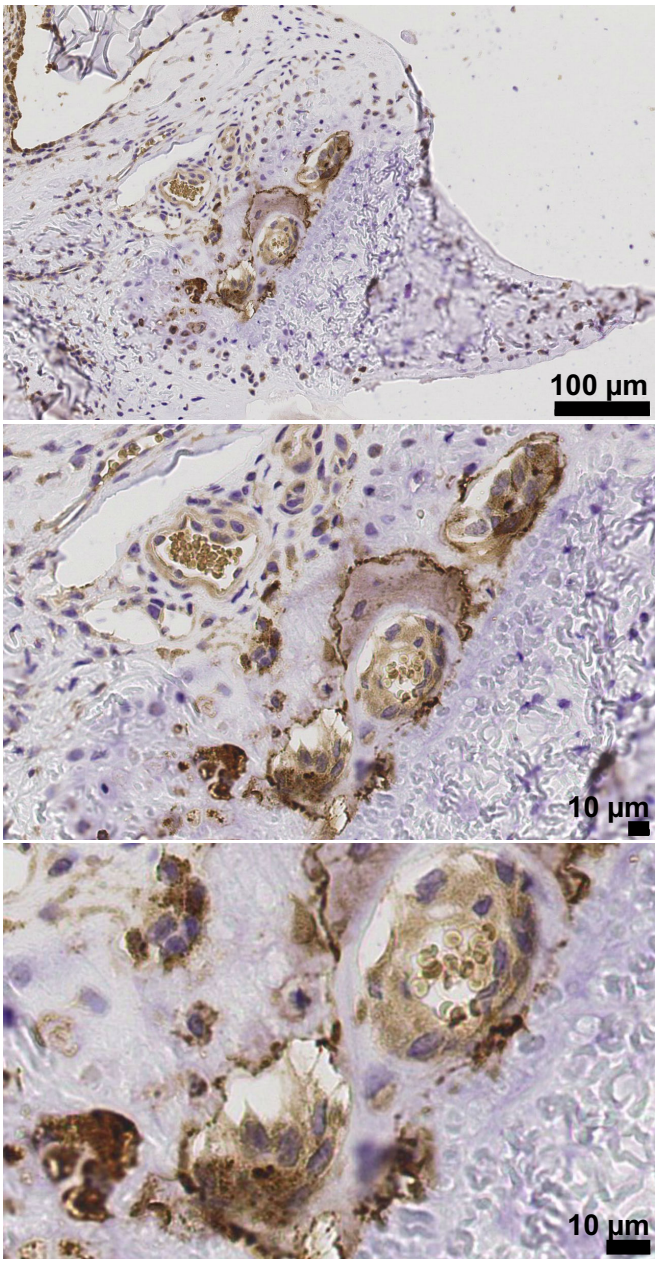

Supplemental Figure 15: Progressively higher magnification images of MMP13 IHC on a representative OA (No Tx) meniscus at 28 days of repetitive loading. Regions of chondroplasia/metaplasia are seen.

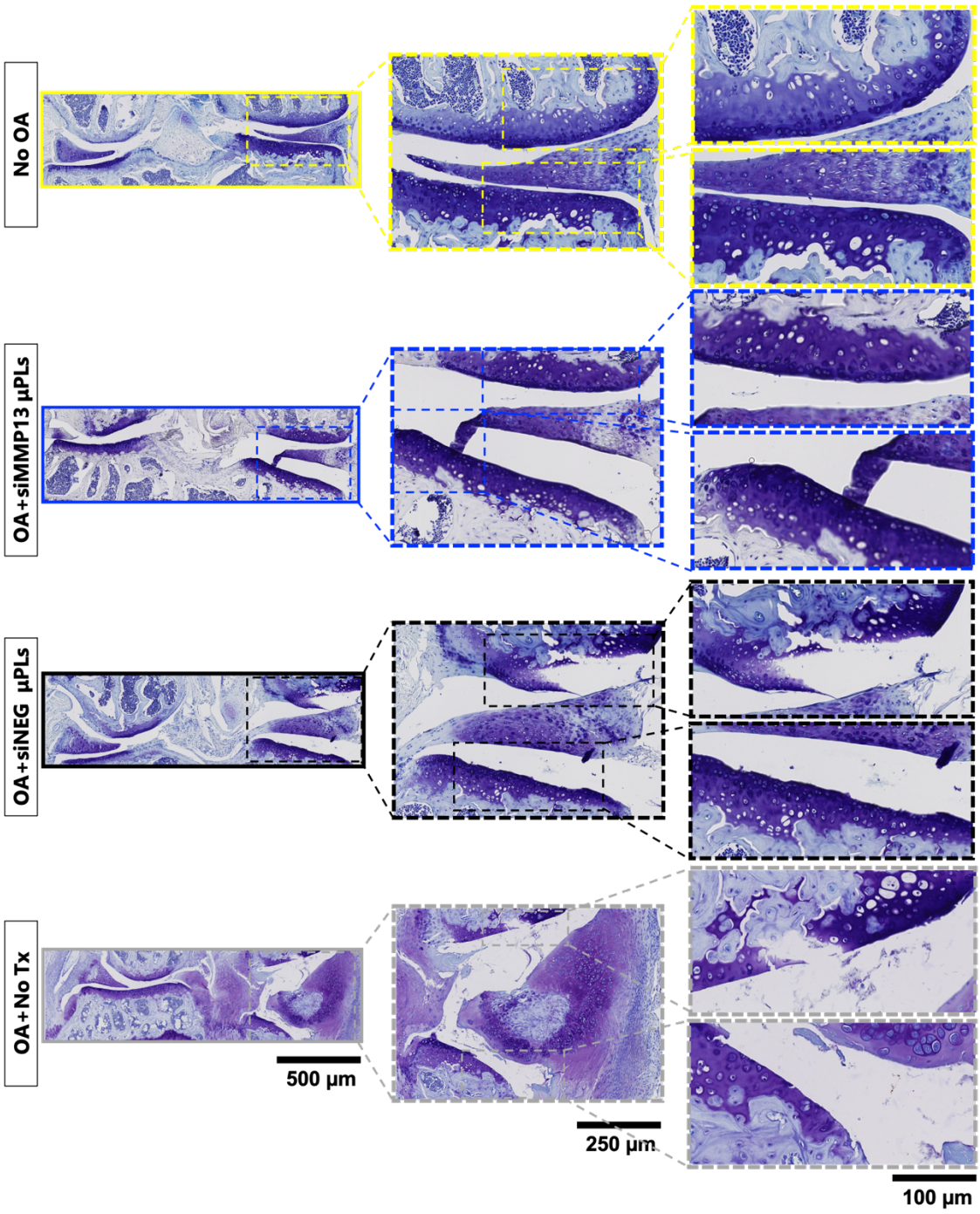

Supplemental Figure 16: Representative Toluidine Blue staining of whole joints, half joints, and femoral and tibial articular cartilage surfaces per treatment group shown as a serial magnification. All images are of knee joints after 4 weeks of repetitive loading and/or initial treatment.

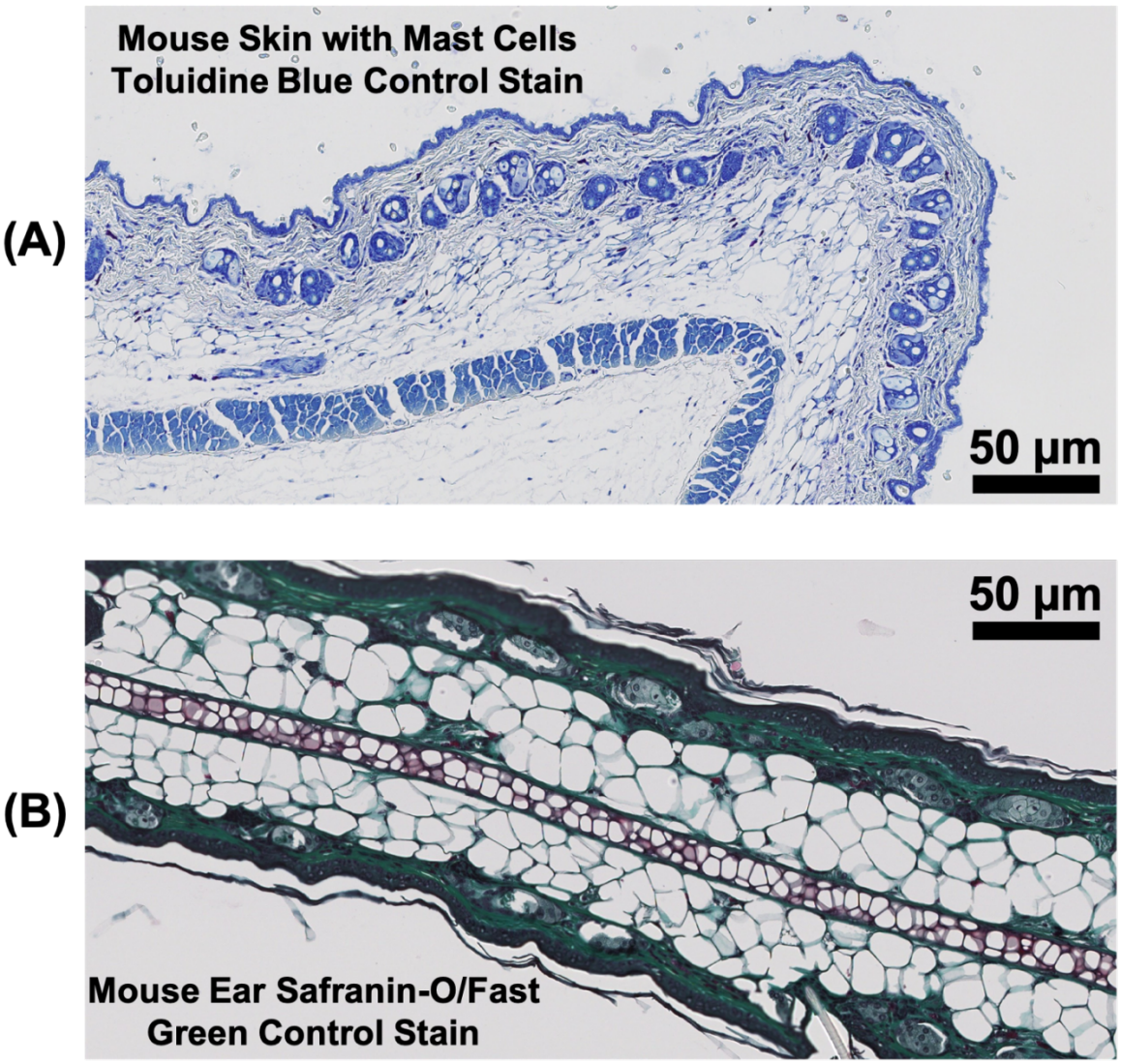

Supplemental Figure 17: (A) Toluidine Blue control stain using mouse skin with mast cells and (B) Safranin-O/Fast Green control stain using mouse ear.

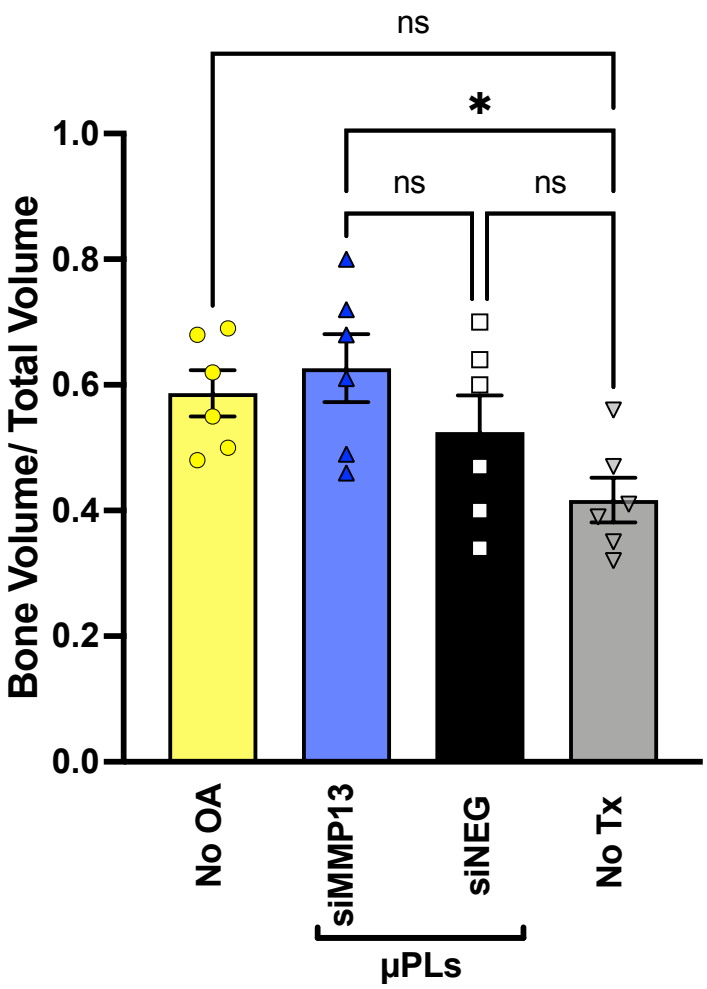

Supplemental Figure 18: Subchondral bone density analysis obtained from MicroCT showing protection of bone architecture by siMMP13-µPLs treatment.